THE HEAT TRANSFORM AND ITS USE IN THERMAL IDENTIFICATION PROBLEMS FOR ELECTRONIC CIRCUITS*

STEFAN KINDERMANN[†] AND MARCIN JANICKI[‡]

Abstract. We define and analyze a linear transformation – the heat transform – that allows to map solutions of hyperbolic equations to solutions of corresponding parabolic equations. The inversion of this mapping can be used to transform an inverse problem for the heat equation to a similar problem for the wave equation. This work is motivated by problems of finding interfaces, boundaries and associated heat conduction parameters in the thermal analysis of electronic circuits when transient data are available. Since the inversion of the transformation is ill-posed, we use a semi-smooth Newton scheme to regularize it enforcing sparsity of the solution. We present some numerical results of this procedure for simulated and measured data, which shows that heat conduction effects due to interfaces and boundaries can be found and classified by an inversion of the heat transform.

Key words. inverse problem, heat transform, sparsity, semi-smooth Newton method, electronic circuits

AMS subject classifications. 35R30, 35K15, 80A23, 44A15, 46F12

1. Introduction. The thermal analysis of electronic systems is a crucial field in modern electronics. An improved understanding of the thermal behavior of semiconductor devices is necessary due to the increased operating frequency and the associated high dissipated power density, which is directly related to the temperature. Reliable thermal circuit models are required to predict system temperature in order to prevent severe damage. The first essential step in building such models is to find from experiments the main heat equation parameters that govern the heat flow.

The stated problem leads to a parameter identification problem for parabolic equations. Such problems are usually nonlinear and often exponentially ill-posed. On the contrary, similar problem associated with hyperbolic equations such as the wave equation are much less ill-posed and, in some circumstances, can even be solved in a stable way, e.g., in tomography. The fundamental difference of the ill-posedness between these two cases is clear from the governing equations: While hyperbolic equations allow transportation of energy and information with finite speed, parabolic equation do not show wave-type behavior, but initial information is smoothed out and can hardly be recovered.

In this paper, we present a new way of analyzing experimental transient temperature data of an electronic system by the use of a linear transformation, the heat transform, which can be used to obtain qualitative information about the associated heat equation parameters, in particular, the location of interfaces and boundaries and the associated heat conduction parameters there.

The main idea of this paper is to relate parabolic equations to hyperbolic equations by the use of the heat transform. This is extremely useful because it allows us to link severely ill-posed inverse problems for the heat equation to similar but mildly ill-posed problem for the wave equation. Since the heat transform is linear, the benefit of our approach is to split a nonlinear severely ill-posed problem into a linear one (inverting the heat transform) and a mildly ill-posed nonlinear one (parameter identification for wave equations). The main difficulty is

thus reduced to a linear inverse problem, for which advanced regularization techniques can be used.

We also note that our work can give a justification to the often used practice of speaking of heat waves that travel through an electronic package. Of course, such a notion does not make sense for parabolic equations, as heat travels with infinite speed. (Note that we do not deal with non-standard heat equations of hyperbolic type, for which heat waves would make sense.) In our approach the heat waves correspond to solutions of the wave equation which can be related to the heat and temperature (using the heat transform) in a mathematically rigorous way.

The central idea of the heat transform introduced in this paper is not new, but is a slight modification (a time integrated version) of the heat transform defined by Widder [24]. It is known that this transform maps the wave equation to the heat equation in the case of classical solutions [5], and this has been used, e.g., in [13, 14]. However, we study this transformation in the more general distributional setting, which is necessary, because solutions of the heat equation need not be classical (at interfaces) or can have singularities, e.g., if the heat source and the measurement point coincide.

To our knowledge such a treatment is new in this context. A standard way of analyzing the thermal properties of electrical circuits is to compute the time-constant spectrum [17, 18] or structure functions [3, 21, 22, 23] from the thermal response data. However, these methods can be seen as model reduction techniques and they suffer from the fact that the computed parameters do not have a real physical interpretation. On the contrary, in our approach, inverting the heat transform yields a wave equation solution, which can be interpreted as reflection waves at interfaces and boundaries. Hence, we can relate the thermal response to a few parameters (the traveling time of the reflected waves), from which the heat conduction parameter or the geometry such as layer thickness can be computed.

The paper is organized as follows: In Section 2, we introduce the partial differential equation of interest and define the heat transform, both for functions and distributions. Furthermore, we show that the proposed transformation maps wave equation solutions to heat equation solutions, cf. Theorems 2.8 and 2.9, which are the main theoretical results. The analysis is done in abstract Hilbert spaces and for distributional solutions. In Section 3, we study some of the properties of the heat transform. Section 3.1 underpins the theoretical result of Theorems 2.8 and 2.9 by an example which also indicates the structure of wave solutions and how parameters can be found by measuring the travel time. In Section 4, we consider the discretization and inversion of the heat transform, for which we use a modified semi-smooth Newton method to enforce the expected sparsity structure. Finally, in Section 5, we present some numerical results using both simulated and experimental data.

2. PDE model and the heat transform. The thermal behavior of an electronic circuit is usually modelled by variants of the heat equation. Data for calibration of thermal models are obtained by the following experiment: one of the active devices or resistors is used to heat the system by a Heaviside power step and the transient thermal response is recorded at one or more locations. Alternatively, the system can be heated first to its thermal steady state and then the cooling curve can be captured.

A large class of electronic systems can be modelled by multi-layer slabs. In this case, the heat source is placed on the top surface and the temperature response is measured at one or several location; see Fig. 2.1. These data are used to determine the relevant heat equation parameters, such as the geometry, the location of layer interfaces, possible defects of the package, or to build reduced thermal models.

In the following we use a quite general PDE description for this: We assume that the heat source strength is constant in time and, thus, the temperature is modelled by the abstract
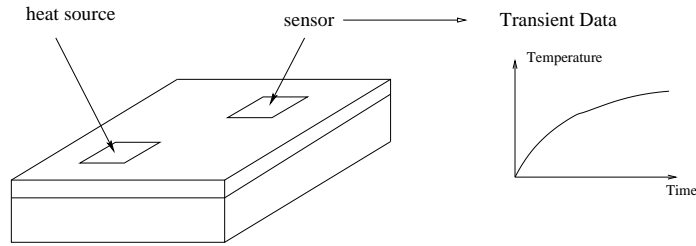
FIG. 2.1. *Experimental setup*

parabolic equation for $u(t, x)$, $t \geq 0$, $x \in \Omega$,

(2.1)
$$\frac{\partial}{\partial t} u = Au + \Theta(t)\chi,$$

were $\Theta(t)$ denotes the Heaviside function

$$\Theta(t) = \begin{cases} 1, & t > 0, \\ 0, & t \leq 0, \end{cases}$$

$\chi(x)$ is a function only depending on the space variable x that describes the shape and location of the source, and A denotes a general time-independent linear second order elliptic partial differential operator together with appropriate boundary conditions. The assumption that A is time-independent is true, if the coefficients in the operator and the boundary conditions are independent of time. Such an assumption is not very restrictive in reality, as long as a linear model is considered.

A standard model for A for the thermal analysis of electrical circuits is the Laplace operator

$$A = D\Delta,$$

where D is the diffusivity depending on the material. If the diffusivity is not constant due to multiple materials, an appropriate operator would be

$$Au = \frac{1}{\rho c} \mathrm{div}(\lambda \nabla u),$$

with the thermal conductivity λ , the density ρ, and the specific heat c. Right now, we do not specify A. The specific structure of A is only relevant when analyzing the heat wave function, but is not needed in the analysis of the heat transform.

We further have to supplement the equation with an initial condition: we assume that u is initially at a constant reference temperature which we can take without loss of generality to be 0. Thus,

(2.2)
$$u(t = 0, x) = 0, \quad x \in \Omega.$$

An observation of a thermal experiment described above yields the thermal profile at some point

$$y(t) := u(t, x_{obs}), \quad t \in \mathbb{R}^+ := \{t > 0\}.$$

A very important task in the thermal analysis of circuits is to find out about the internal structure of the electronic system from such thermal measurements y. This can serve for

several purposes, for instance, to determine thermal parameters (e.g., thermal diffusivity, conductivity, heat transfer coefficients, boundary conditions, etc.), to improve modelling of the circuit or for model reduction, by building a simpler model of the circuit which have similar thermal response.

A common way to analyse the thermal response is to calculate the so-called *time-constant spectrum* [22], $\tilde{R}(\tau)$, defined as

$$(2.3) \qquad y(t) =: \int_0^\infty \tilde{R}(\tau)(1 - \exp(-\frac{t}{\tau}))d\tau.$$

An alternative version of the time constant spectrum uses a change of variables $\tau = \exp(\xi)$ and $R(\xi) = \tilde{R}(\exp\xi)\exp\xi$. In this case R is given by [22]

$$(2.4) \qquad y(t) =: \int_{-\infty}^\infty R(\xi)(1 - \exp(-\frac{t}{\exp(\xi)}))d\xi.$$

Based on this, further transformation can be made to find another representation of the system, such as the *structure function* [3, 21, 22, 23].

The time-constant spectrum completely determines the thermal system in a specific configuration, but it has a drawback: it is not clear, how the information in R is related to any real geometric structure of the package. It would be advantageous to directly infer form the data some information about the internal structure of the package, such as interfaces, cooling or heat-transfer parameters. Right now, such information is extracted from $\tilde{R}$ on a more or less heuristic basis drawn from experience. Some more rigorous attempts using the time-constant spectrum have been made by relating the structure function to a one-dimensional heat flow model [3], but the validity of this simplified model in more general, non symmetric situations is not clear.

In order to circumvent this drawback, we propose to compute a different function – the heat wave function – instead of the time-constant spectrum. This allows us to directly find out about the internal structure of the package, as long as we can make sense out of the solution of the wave equation corresponding to the operator A.

Associated to (2.1) we define the following heat wave function $w(s, x)$, $s \geq 0$, $x \in \Omega$, as a weak solution of the wave equation

$$(2.5) \qquad \frac{\partial^2 w}{\partial s^2} = Aw + \delta(s)\chi,$$

supplemented with zero Cauchy data

$$(2.6) \qquad w(s = 0, x) = 0, \quad \frac{\partial}{\partial s}w(s = 0, x) = 0, \quad x \in \Omega.$$

Here δ is the delta-distribution centered at 0. Alternatively, we can define w as solution of (2.5) on $\mathbb{R} \times \Omega$ together with the condition that $w(s, x) = 0$ for $s \leq 0$, or in other words, that the support of w is contained in the positive s-axis.

Now the main idea is to find a transformation that relates u to w. This transformation is central to our analysis and we will refer to it as the heat transform. We first define it for real-valued functions.

DEFINITION 2.1. *The* heat transform *is the linear transformation, that maps a function* $w : \mathbb{R}^+ \to \mathbb{R}$ *to the function* $\mathcal{H}w(t)$

$$(2.7) \qquad \mathcal{H}w(t) := \int_0^\infty w(s)\Phi(\frac{s}{2\sqrt{t}})ds,$$

whenever the integral exists. Here Φ is the complementary error function

$$\Phi(x) := erfc(x) := \frac{2}{\sqrt{\pi}} \int_x^\infty e^{-\tau^2} d\tau.$$

Of course, the definition only makes sense, when the integral exists. The heat wave function w is not necessarily a function, but rather a distribution. The extension of definition (2.7) to distributions is obvious, if we only do formal calculations: if w is a distribution in $\mathcal{S}'(\mathbb{R})$, then formally we could define its heat transform by the duality paring

$$(\mathcal{H}w)(t) := \langle w, \Phi(\frac{\cdot}{2\sqrt{t}}) \rangle_{\mathcal{S}',\mathcal{S}}. \quad t > 0.$$

We did not specify this equation as a definition, because it is not clear that the right-hand side exists, because $\Phi(\frac{\cdot}{2\sqrt{t}})$ is not in $\mathcal{S}(\mathbb{R})$. However, it certainly exists for distributions with compact support (see [12, Thm 2.3.1]), and for $t > 0$. For tempered distributions $\mathcal{S}'$ with support in $\mathbb{R}^+$, we can define the heat transform by using an appropriate cutoff-function:

DEFINITION 2.2. *Let $w \in \mathcal{S}'(\mathbb{R})$ with support in $\mathbb{R}^+$. Let $\psi(s) \in C^\infty(\mathbb{R})$ a cutoff function, which is 1 in a neighborhood of $supp(w)$, and 0 for $s < -s_0 < 0$, for some $s_0 \in \mathbb{R}^+$. Then the heat transform is defined as*

$$(2.8) \qquad\qquad \mathcal{H}w(t) := \left\langle w, \psi(.)\Phi\left(\frac{\cdot}{2\sqrt{t}}\right) \right\rangle_{\mathcal{S}',\mathcal{S}},$$

for $t > 0$.

This definition makes sense as we show in the following lemma.

LEMMA 2.3. *With ψ as in definition (2.2), and for $t > 0$ fixed, $\psi(.)\Phi(\frac{\cdot}{2\sqrt{t}})$ is in $\mathcal{S}(\mathbb{R})$.*

Proof. By induction it is immediate that

$$(2.9) \qquad\qquad \frac{\partial^k}{\partial s^k}\Phi(\frac{s}{2\sqrt{t}}) = e^{\frac{-s^2}{4t}} p_{k-1}(\frac{s}{\sqrt{t}})\frac{1}{t^{\frac{k}{2}}}, \quad k \geq 1,$$

with a polynomial p_{k-1} of degree $k - 1$. Thus, all derivatives of order $k > 0$ are rapidly decaying functions for $t > 0$. However, $\lim_{s \to -\infty} \Phi(\frac{s}{2\sqrt{t}})$ is not decaying, but due to the multiplication with the cutoff-function the decay is established. The definition of $\mathcal{H}w$ does not depend on the choice of the cutoff-function, by the definition of the support. ☐

Note that at $t = 0$ the function $\Phi(\frac{s}{2\sqrt{t}})$ has a jump singularity at $s = 0$, so the heat transform is not well defined for distributions at $t = 0$. However, if we would like to be $\mathcal{H}w$ a solution to a heat equation, we have to be able to use values at $t = 0$, to state initial conditions. We will remedy this situation by using a small time-shift $\epsilon > 0$ and then let ϵ tend to 0; see (2.14) below.

We intend to show that the wave equation solution and the heat equation solution are related by the heat transform. Here, some care has to be taken, since the heat wave function is typically a distribution, so we have to use an appropriate weak solution. A weak solution of (2.5), (2.6) will be a tempered distribution on $\mathbb{R}$ with values in a separable Hilbert space V (see, e.g., [25]):

$$w : \mathcal{S}(\mathbb{R}) \to V, \quad \text{in symbol: } w \in \mathcal{S}'(\mathbb{R}; V).$$

That is, for any $\phi \in \mathcal{S}$, the mapping

$$\mathcal{S}(\mathbb{R}) \to V$$
$$\phi \to \langle w(., x), \phi(.) \rangle_{\mathcal{S}'(\mathbb{R}), \mathcal{S}(\mathbb{R})}$$

is linear and continuous.

Moreover, we assume that the operator A induces a continuous bilinear form on $V \times V$:

$$(2.10) \qquad a(u,v) := -(Au, v) \quad \text{bilinear and continuous } V \times V \to \mathbb{R}.$$

Now let $w(s,x)$ be a classical solution such that $w(s,.)$ is twice differentiable with values in V. Then multiplying (2.5) by a test function and integrating, we obtain a weak formulation in the usual way (compare, e.g., [8]):

$$\frac{\partial^2}{\partial s^2}(w(s,.), v)_{V',V} + a(w(s,.), v) = \delta(s)(\chi, v)_{V',V}.$$

Let η_i be an orthonormal basis of V. Then we can express w in the form

$$w(s,x) = \sum_{i=1}^{\infty} \zeta_i(s)\eta_i(x),$$

and obtain

$$(2.11) \qquad \sum_{i=1}^{\infty} \frac{\partial^2}{\partial s^2}\zeta_i(s)\,(\eta_i, v)_{V',V} + \zeta_i(s)a(\eta_i, v) = \delta(s)(\chi, v)_{V',V}.$$

This identity holds, because the series for w converges in V and the bilinear form is continuous on V. Now this reasoning leads to an appropriate definition of a weak solution: we only have to replace ζ_i by tempered distributions and consider equation (2.11) in $\mathcal{S}'$.

DEFINITION 2.4. *By a weak solution to* (2.5) *we mean a V-valued distribution $\mathcal{S}'(\mathbb{R}; V)$ with an expansion*

$$(2.12) \qquad w(s,x) = \sum_{i=1}^{\infty} \zeta_i(s)\eta_i,$$

where η_i is an orthonormal basis of V and $\zeta_i \in \mathcal{S}'(\mathbb{R})$, such that $\forall \phi \in \mathcal{S}(\mathbb{R})$, $\forall v \in V$,

$$\sum_{i=1}^{\infty} \left\langle \frac{\partial^2}{\partial s^2}\phi, \zeta_i \right\rangle (\eta_i, v)_{V',V} + \langle \zeta_i, \phi \rangle\, a(\eta_i, v) = \langle \delta, \phi \rangle\, (\chi, v)_{V',V},$$

such that all ζ_i have support in $\mathbb{R}^+$. The support condition is the appropriate formulation of zero initial data (2.6). From the derivation it should be clear that a classical solution is also a weak solution.

We now have to define the heat transform for functions in $\mathcal{S}'(\mathbb{R}; V)$.

DEFINITION 2.5. *Let $w \in \mathcal{S}'(\mathbb{R}, V)$ with support in $\mathbb{R}^+$. Then*

$$(2.13) \qquad (\mathcal{H}w)(t) := \langle w, \Phi(\frac{\cdot}{2\sqrt{t}}) \rangle, \quad t > 0,$$

or equivalently, if w has an expansion as in (2.12)*, then*

$$(\mathcal{H}w)(t) = \sum_{i=1}^{\infty}(\mathcal{H}\zeta_i)(t)\,\eta_i.$$

Note that the integral in this definition (2.13) is a Bochner integral [25]. As we have indicated, we have to consider the value of $(\mathcal{H}w)(t)$ at $t = 0$. This is a subtle point due to possible singularities. We therefore need an approximated version of the heat transform:

DEFINITION 2.6. *Let* $w \in \mathcal{S}'(\mathbb{R}, V)$ *or let* $w \in \mathcal{S}'(\mathbb{R})$ *with support in* $\mathbb{R}^+$. *Then for any* $\epsilon > 0$, *we define*

$$(2.14) \qquad (\mathcal{H}_\epsilon w)(t) := \langle w(\, . - \epsilon), \Phi(\frac{\cdot}{2\sqrt{t}}) \rangle = \langle w, \Phi(\frac{\cdot + \epsilon}{2\sqrt{t}}) \rangle, \quad t > 0.$$

The approximate transform has well-defined values at $t = 0$. Moreover, if w has support in $s > 0$, then as $\epsilon \to 0$, the approximate heat transform $\mathcal{H}_\epsilon$ converges to $\mathcal{H}$:

LEMMA 2.7. *Let* $w \in \mathcal{S}'(\mathbb{R})$ *with support in* $\mathbb{R}^+$. *Then* $\phi_\epsilon(t) := (\mathcal{H}_\epsilon w)(t)$ *is a* $C^\infty(]0, \infty[)$*-function with*

$$\lim_{t \to 0} \frac{d^k}{dt^k} \phi_\epsilon(t) = 0 \quad \forall k \in \mathbb{N}.$$

If $w \in \mathcal{S}'(\mathbb{R})$ *with support in* $\{s \in \mathbb{R} \,|\, s > 0\}$, *then*

$$\mathcal{H}w(t) = \lim_{\epsilon \to 0} (\mathcal{H}_\epsilon w)(t)$$

for all $t > 0$.

Proof. Note that $w(. - \epsilon)$ is in $\mathcal{S}'(\mathbb{R})$ and has support in $[\epsilon, \infty[$. Since $\Phi(\frac{\cdot}{2\sqrt{t}})$ is in C^∞ for $t > 0$, $\mathcal{H}_\epsilon$ is well defined. Moreover, from (2.9) it follows that on $[\epsilon, \infty[$, $\lim_{t \to 0} \Phi(\frac{\cdot}{2\sqrt{t}}) = 0$ in $C^\infty([\epsilon, \infty[)$. Moreover, the same holds for $\frac{d^k}{dt^k}\Phi(\frac{\cdot}{2\sqrt{t}})$, which establishes the proof of the first part. For the second part we observe that $\Phi(\frac{\cdot + \epsilon}{2\sqrt{t}})$ converges to $\Phi(\frac{\cdot}{2\sqrt{t}})$ in $C^\infty([\tau, \infty[)$ for any positive τ as $\epsilon \to 0$. Since the support of w is contained in an interval $[\tau, \infty[$ this suffices for convergence; cf. [12, Thm 2.3.1]. $\square$

We now come to the main theorem: We postulate the existence of a weak solution to the wave equation and conclude that its heat transform satisfies the heat equation. The only assumption on A is that the induced bilinear form is continuous and time-independent.

THEOREM 2.8. *Let* $w : \mathcal{S}'(\mathbb{R}) \to V$ *be a weak solution of the wave equation* (2.5), *and* (2.6) *as in Definition* 2.4. *Assume that the bilinear form* $a(.,.)$ *satisfies* (2.10) *and does not depend on time. Let*

$$u_\epsilon := \mathcal{H}_\epsilon w.$$

Then u_ϵ *is in* $C^\infty([0, T], V)$ *for any* $T > 0$ *and satisfies*

$$\frac{d}{dt}(u_\epsilon, v)_{V', V} + a(u_\epsilon, v) = \Phi(\frac{\epsilon}{2\sqrt{t}})(\chi, v)_{V', V} \quad \forall v \in V, t > 0.$$

Moreover,

$$(2.15) \qquad \lim_{t \to 0} u_\epsilon(t, .) = 0.$$

Proof. A direct calculation shows that for $t > 0$, $\Phi(\frac{s}{2\sqrt{t}})$ satisfies

$$(2.16) \qquad \frac{\partial}{\partial t}\Phi(\frac{s}{2\sqrt{t}}) = \frac{\partial^2}{\partial s^2}\Phi(\frac{s}{2\sqrt{t}}).$$

Now assume that $w \in \mathcal{S}'(\mathbb{R}; V)$ is a weak solution to (2.5) and (2.6). Since the support of $w(. - \epsilon)$ is in $[\epsilon, \infty[$, and because of (2.9), a difference approximation to $\frac{d}{dt}\mathcal{H}_\epsilon w(t) \sim \frac{\Delta}{\Delta t}\mathcal{H}_\epsilon w$

equals $\langle w(. - \epsilon), \frac{\Delta}{\Delta t}\Phi(\frac{\cdot}{2\sqrt{t}})\rangle$. The limit $\Delta t \to 0$ will converge in $\mathcal{S}'$ to $\langle w(. - \epsilon), \frac{\partial}{\partial t}\Phi(\frac{\cdot}{2\sqrt{t}})\rangle$, because of the support of w. Together with (2.16) this yields

$$\frac{d}{dt}\mathcal{H}_\epsilon w(t) = \left\langle w(. - \epsilon), \frac{\partial^2}{\partial \tau^2}\Phi(\frac{\cdot}{2\sqrt{t}})\right\rangle = \mathcal{H}_\epsilon(\frac{\partial^2}{\partial \tau^2}w),$$

by the definition of distributional derivative. Since w satisfies equation (2.11) and $a(.,.)$ does not depend on t, it is obvious that $w(. - \epsilon)$ satisfies the same equation but with $\delta(t)$ replaced by $\delta(. - \epsilon)$. Thus,

$$\frac{d}{dt}\mathcal{H}_\epsilon w(t) + \sum_{i=1}^{\infty}\langle\mathcal{H}_\epsilon\zeta_i\rangle \, a(\eta_i, v)$$

$$= \left(\delta(. - \epsilon), \Phi(\frac{\cdot}{2\sqrt{t}})\right)(\chi, v)_{V',V} = \Phi(\frac{\epsilon}{2\sqrt{t}})(\chi, v)_{V',V}.$$

Note that for $t \geq 0$, $\sum_{i=1}^{\infty}(\mathcal{H}_\epsilon\zeta_i)\eta_i$ is an element in V by definition of $\mathcal{S}'(\mathbb{R}, V)$ and

$$\|\sum_{i=1}^{\infty}(\mathcal{H}_\epsilon\zeta_i)(t)\eta_i\|^2 = \sum_{i=1}^{\infty}|\mathcal{H}_\epsilon\zeta_i)(t)|^2 = \|(w(. - \epsilon), \Phi(\frac{\cdot}{2\sqrt{t}}))\|^2 \leq C,$$

which shows that the series converges. Because of the continuity of a, we obtain

$$\sum_{i=1}^{\infty}(\mathcal{H}_\epsilon\zeta_i)(t)a(\eta_i, v) = a(\mathcal{H}_\epsilon w(t), v).$$

The uniform boundedness of $\|u_\epsilon(t, .)\|_V$ and of all its time-derivatives for any t in $[0, T]$ follows by the same arguments, hence, $u_\epsilon \in C^\infty([0, T], V)$. Equation (2.15) follows from the first part of Lemma 2.7. $\square$

We have seen that the approximate heat transform satisfies a heat equation similar to (2.1). We can now take the limit $\epsilon \to 0$. In view of Lemma 2.7, u_ϵ will converge to the heat transform if the assumptions of this lemma apply. If they are not satisfied, the pointwise limit does not exist, but we can show the limit exists in an appropriate Banach space. For this we rely on well-known estimates for parabolic equations assuming that the operator A is uniformly elliptic:

THEOREM 2.9. *Let $V \subset H \subset V'$ be a Gelfand triple, let $a(.,.)$ be as in Theorem 2.8, and additionally let a Garding inequality hold:*

$$a(u, u) + k_0\|u\|_H^2 \geq \alpha\|u\|_V^2 \quad \forall u \in V,$$

for some constants $\alpha > 0$, $k_0 \geq 0$. Moreover, assume that $\chi \in V'$. Then

$$u := \lim_{\epsilon \to 0} u_\epsilon$$

exists in $L^2([0, T], V)$ for all $t > 0$ and satisfies the heat equation (2.1) in a weak form

$$\frac{d}{dt}(u, v)_{V',V} + a(u, v) = \Theta(t)(\chi, v)_{V',V} \quad \forall v \in V$$

with zero initial data.

Proof. We already know that u_ϵ satisfies the heat equation with right-hand side $\Phi(\frac{\epsilon}{2\sqrt{t}})$ in place of $\Theta(t)$. According to standard parabolic estimates the weak solution depends continuously in the $L^2([0,T];V)$-norm on the $L^2([0,T];V')$-norm of the right-hand side. Now as $\epsilon \to 0$,

$$\Phi(\frac{\epsilon}{2\sqrt{t}}) \to \begin{cases} 1, & t > 0, \\ 0, & t = 0, \end{cases}$$

pointwise for all t. Since $\Phi(\frac{\epsilon}{2\sqrt{t}}))$ is bounded by a constant and $\chi \in V'$, the dominated convergence theorem shows that

$$\Phi(\frac{\epsilon}{2\sqrt{t}})(\chi,.) \to \Theta(t)(\chi,.) \quad \text{in } L^2([0,T];V'),$$

which proves the assertion. $\square$

This theorem provides the theoretical basis for the use of the heat transform. From Theorem 2.9 and Lemma 2.7, we can conclude that solutions $w(s,x)$ to the wave equation (2.5) and solutions to the heat equations $u(t,x)$ are related by

$$(2.17) \qquad u(.,x) = \mathcal{H}w(.,x).$$

When we are given thermal measurements satisfying (2.1), we can try to compute the underlying wave equation solution by inverting $\mathcal{H}$. This heat wave function will -as in tomography-contain much information on the internal structure of the package. The inverse problem of finding internal parameter for the heat equation is then reduced to the corresponding problem for the wave equation, which is less ill-posed.

3. Properties of the heat transform. We now show some elementary properties of $\mathcal{H}$.

PROPOSITION 3.1. *Let $w(s)$ be an integrable function on $\mathbb{R}^+$ (i.e., $w \in L^1(\mathbb{R}^+)$). Then $\mathcal{H}w(t)$ is defined for all $t > 0$ and bounded. Then it holds that*

$$(3.1) \qquad \lim_{t \to 0} \mathcal{H}w(t) = 0,$$

$$(3.2) \qquad \lim_{t \to \infty} \mathcal{H}w(t) = \int_0^\infty w(s)ds.$$

If, additionally $\frac{d^2}{ds^2}w(s)$ is integrable, then $\mathcal{H}w(t)$ is differentiable for $t > 0$ and

$$(3.3) \qquad \frac{d}{dt}\mathcal{H}w(t) = \mathcal{H}(\frac{d^2}{ds^2}w)(t) + \frac{1}{\sqrt{\pi t}}w(0) + \frac{d}{ds}w(0).$$

Proof. As Φ is always bounded, and if w is integrable, the integral exists. The assertions (3.1), (3.2) follow from the dominated convergence theorem if we notice that pointwise

$$\lim_{t \to 0} \Phi(\frac{s}{2\sqrt{t}}) = \begin{cases} 0, & s > 0, \\ 1, & s = 0, \end{cases} \qquad \lim_{t \to \infty} \Phi(\frac{s}{2\sqrt{t}}) = 1, \ \forall s \geq 0.$$

For (3.3) we notice that (2.16) is satisfied for all $t > 0$. Moreover, the integral $\int_0^\infty w(s)\frac{\partial^2}{\partial s^2}\Phi(\frac{s}{2\sqrt{t}})ds$ converges as above. Thus, integration by parts yields

$$\int_0^\infty w(s)\frac{\partial^2}{\partial s^2}\Phi(\frac{s}{2\sqrt{t}})ds = \int_0^\infty \frac{\partial^2}{\partial s^2}w(s)\Phi(\frac{s}{2\sqrt{t}})ds$$

$$+w(s)\frac{\partial}{\partial s}\Phi(\frac{s}{2\sqrt{t}})|_{s=0}^{\infty} - \frac{\partial}{\partial s}w(s)\Phi(\frac{s}{2\sqrt{t}})|_{s=0}^{\infty}.$$

The limits of $w(s), \frac{\partial}{\partial s}w(s)$ at $s \to \infty$ vanish due to our assumptions, the limits at $s = 0$ yield (3.3). Note that $\frac{\partial}{\partial s}w(0)$ exists, due to Sobolev's embedding theorem.   □

Equation (3.1) is consistent with the zero initial conditions imposed on the temperature. Equation (3.2) is more interesting, as it allows us to compute the total temperature increase $u(\infty, x_{obs}) - u(0, x_{obs})$ by the integral over the wave function.

Since an alternative derivation of the heat transform could be done (at least formally) by the Laplace-transform, we state the main property of $\mathcal{H}$ under the Laplace transform:

PROPOSITION 3.2. *Define the Laplace transform*

$$\mathcal{L}(f)(\tau) := \int_0^{\infty} e^{-\tau t}f(t)dt$$

and let $w(\tau)$ be integrable, then

(3.4)
$$\mathcal{L}(\mathcal{H}w)(\tau) = \frac{1}{\tau}\mathcal{L}(w)(\sqrt{\tau}) \quad \forall \tau > 0.$$

Proof. Since $\mathcal{H}w$ is bounded, its Laplace transform exists.

$$\mathcal{L}(\mathcal{H}w)(\tau) = \int_0^{\infty}\int_0^{\infty} e^{-\tau t}\Phi(\frac{s}{2\sqrt{t}})w(s)dsdt.$$

Because $w(s)e^{-\tau t}$ is $d(s,t)$ integrable and Φ is bounded, an application of Fubini's theorem leads to

$$\mathcal{L}(\mathcal{H}w)(\tau) = \int_0^{\infty}\int_0^{\infty} e^{-\tau t}\Phi(\frac{s}{2\sqrt{t}})dtw(s)ds.$$

A calculation of the inner integral - either using computer algebra or by integration by parts and with formula [9, 3.472.3] – yields for $s > 0$,

$$\int_0^{\infty} e^{-\tau t}\Phi(\frac{s}{2\sqrt{t}})dt = \frac{1}{\tau}e^{-s\sqrt{\tau}}.$$

The same holds for $s = 0$. This proves the result.   □

If we apply the Laplace transform to the heat and wave equations, then this again shows that solutions of the heat equation and the wave equation are related via the heat transform. In the Laplace domain, $\sqrt{\tau}$ in (3.4) is the factor responsible for changing the second derivative in (2.5) to the first derivative in (2.1), while $\frac{1}{\tau}$ deals with the change of the delta-distribution on the right-hand side in (2.5) to the Heaviside function in (2.1).

We now compare the heat transform to the time-constant spectrum. The following result states that the time-constant spectrum can be calculated from the heat wave function:

THEOREM 3.3. *Let $w(s), \frac{d^2}{ds^2}w(s)$ be integrable and $\frac{d}{ds}w(\infty) = w(0) = 0$. Furthermore, let $s\frac{d^2}{ds^2}w(s)$ be integrable as well. If $\tilde{R}(\tau)$ is defined as*

$$\tilde{R}(\tau) = \int_0^{\infty} \frac{1}{\pi}\sin(\frac{s}{\sqrt{\tau}})\frac{1}{\tau}w(s)ds$$

and $y(t)$ is defined by (2.3), then for $t > 0$,

$$y(t) = \mathcal{H}w(t).$$

Proof. The integral exists and is bounded for any $\tau > 0$. The limit as $\tau \to 0$ can be computed by integration by parts, and due to the assumptions,

$$-\tilde{R}(\tau) = \frac{1}{\pi} \int_0^\infty \frac{d2}{ds^2} \sin(\frac{s}{\sqrt{\tau}}) w(s) ds = \frac{1}{\pi} \int_0^\infty \sin(\frac{s}{\sqrt{\tau}}) \frac{d2}{ds^2} w(s) ds$$

$$-\frac{1}{\pi} \sin(\frac{s}{\sqrt{\tau}}) \frac{d}{ds} w(s)|_0^\infty + \frac{1}{\pi\sqrt{\tau}} \cos(\frac{s}{\sqrt{\tau}}) w(s)|_0^\infty = \frac{1}{\pi} \int_0^\infty \sin(\frac{s}{\sqrt{\tau}}) \frac{d2}{ds^2} w(s),$$

which shows that $\tilde{R}(\tau)$ is uniformly bounded for $\tau \in [0, \infty]$. Hence, the integral in (2.3) exists. Thus,

$$y(t) = \int_0^\infty \int_0^\infty (1 - e^{-\frac{t}{\tau}}) \frac{1}{\pi} \sin(\frac{s}{\sqrt{\tau}}) \frac{1}{\tau} w(s) ds d\tau$$

$$= -\frac{1}{\pi} \int_0^\infty \int_0^\infty (1 - e^{-\frac{t}{\tau}}) \sin(\frac{s}{\sqrt{\tau}}) \frac{d2}{ds^2} w(s) ds d\tau.$$

For the following integral, we use that $\sin(s) \leq s$, for $s \geq 0$,

$$\int_0^\infty |\sin(\frac{s}{\sqrt{\tau}})| |\frac{d2}{ds^2} w(s)| ds \leq \frac{1}{\sqrt{\tau}} \int_0^\infty s |\frac{d2}{ds^2} w(s)| ds \leq C \frac{1}{\sqrt{\tau}}.$$

This shows that the iterated integral

$$\int_0^\infty \int_0^\infty |(1 - e^{-\frac{t}{\tau}}) \sin(\frac{s}{\sqrt{\tau}}) \frac{d2}{ds^2} w(s)| ds d\tau$$

exists. By Tonelli's theorem we can switch integration and with (see [9, 3.952.6])

$$\int_0^\infty (1 - e^{-\frac{t}{\tau}}) \frac{1}{\pi} \sin(\frac{s}{\sqrt{\tau}}) \frac{1}{\tau} d\tau = \Phi(\frac{s}{2\sqrt{t}}),$$

the result follows.   □

Since the transform of w to $\tilde{R}$ is given as an integral equation, we conclude that the problem of computing the time-constant spectrum from the heat wave function is a well posed problem (in appropriate spaces), while the converse - finding the w from $\tilde{R}$ is an ill-posed problem, as it involves the inversion of an integral equation.

If we use (2.4), then the time-constant spectrum can be computed (at least formally) by a convolution. Indeed, after a change of coordinates

$$s = \exp \frac{\eta}{2}, \qquad \bar{w}(\eta) := w(\exp \frac{\eta}{2}) \exp \frac{\eta}{2},$$

$$R = \frac{1}{2\pi} \int_{-\infty}^\infty \sin(\exp(\frac{\xi - \eta}{2})) \bar{w}(\eta) d\eta.$$

3.1. Example. We now turn to an example which shows the advantages of the heat transform. Consider the temperature in a 3D-block $\Omega = [-1, 1]^3$. The temperature u is assumed to satisfy the heat equation as in (2.1),

(3.5) $$\frac{\partial}{\partial t} u(t, x) = D\Delta u + \Theta(t)\chi(x),$$

together with zero initial condition and homogenous Neumann conditions,

$$u(0, x) = 0, \quad x \in \Omega, \qquad \frac{\partial}{\partial n} u(t, x) = 0, \quad x \in \partial\Omega.$$

We now look at the corresponding heat wave function. According to our analysis it must satisfy

(3.6) $$\frac{\partial^2}{\partial s^2} w(s, x) = D\Delta w(s, x) + \delta(s)\chi(x),$$

together with zero Cauchy data at $t = 0$ and the same boundary conditions as u. We further assume that the source at $x = 0$ is very small such that we can approximate it by a delta function centered at $x = 0$:

$$\chi(x) = \delta(x).$$

By the reflection principle, we can remove the boundary conditions by putting artifical sources outside Ω that mirror the source at the boundary. The location of these source is at $(x, y, z) = (2i, 2j, 2k)$, where $i, j, k \in \mathbb{Z}$. Then $w(s, x)$ satisfies

$$\frac{\partial^2}{\partial s^2} w(s, x) = D\Delta w(s, x) + \delta(s) \sum_{i,j,k=-\infty}^{\infty} \delta(x - (2i, 2j, 2k)), \quad \text{in } \mathbb{R}^3 \times \mathbb{R}^+,$$

where the initial conditions are the same. The solution w is a superposition of fundamental solutions to the wave equation, where the fundamental solutions have support in $s \geq 0$. Note that the diffusivity of the heat equation plays the role of the squared wave speed $D = c^2$: The fundamental solution to (3.6) is well known, in fact if $\chi = \delta(x - x_{source})$, then the fundamental solution $w(s, x)$ is the distribution [6]:

$$w(s, x) = \frac{1}{4\pi D|x_{source} - x|} \delta\left(t - \frac{|x_{source} - x|}{\sqrt{D}}\right).$$

As mentioned above, the solution to (3.6) is a superposition of fundamental solutions at points $z_{i,j,k} := (2i, 2j, 2k)$. Thus if we observe at $x = x_{obs}$,

$$w(s, x_{obs}) = \sum_{(i,j,k) \in \mathbb{Z}^3} \frac{1}{4\pi D|x_{source} - z_{i,j,k} - x_{obs}|} \delta\left(s - \frac{|x_{source} - z_{i,j,k} - x_{obs}|}{\sqrt{D}}\right).$$

We see that the wave equation solution is a superposition of delta-distributions with decreasing intensity. The shift and intensity depends on the distance of the observer to the source.

Let us now observe the temperature at a point x_{obs}. According to Theorem 2.9, u is related to w by the heat transform:

$$u(t, x_{obs}) = \mathcal{H}w(., x_{obs})(t).$$

If we compute the heat transform for $w(s, x_{obs})$, we obtain

(3.7) $$u(t, x_{obs}) = \sum_{i,j,k} \frac{1}{4\pi D|x_{source} - z_{i,j,k} - x_{obs}|} \Phi\left(\frac{|x_{source} - z_{i,j,k} - x_{obs}|}{\sqrt{4tD}}\right).$$

This is exactly the solution to the heat equation. Indeed, if we use the Green's function for the heat equation,

$$G(x, t; y) = \frac{1}{(4\pi tD)^{\frac{3}{2}}} e^{-\frac{|x-y|^2}{4Dt}},$$

and again the reflection principle, then we can compute the solution to (3.5),

$$u(t, x_{obs}) = \sum_{i,j,j} \int_0^t G(x_{obs}, t - s; z_{i,j,k}) ds.$$

Now by elementary integration this is exactly (3.7).

This examples shows, that if the wave equation solution is known (it can be computed from $u(t, x_{obs})$ by inverting the heat transform), then one can, for instance, find either the location of the source or the diffusivity. In fact, if the location of the first pulse is found at s_{puls}, then

(3.8) $$s_{puls} = \frac{|x_{obs} - x_{source}|}{\sqrt{D}},$$

which gives an easy formula to compute either the distance to the source or the diffusivity if one of them is known. On the contrary, it is not easy to find these parameters directly from $u(t, x_{obs})$.

Let us mention, that the amplitudes of the pulses can be negative. This happens, if we replace the Neumann boundary condition by Dirichlet boundary conditions $u(t, x) = 0$ on $\partial\Omega$. The reflection principle is similar then, but the reflected sources have to be taken with a negative sign.

Of course, further information can be obtained as well. Note that at boundaries between materials, one part of the wave is reflected and another part is refracted. The reflected wave can be seen at the observation point, from which the location of the interface can be computed.

From this example we also recognize that the heat transform maps the Green's function of the wave equation to the time-integrated Green's function of the heat equation. From the representation of general solutions by the Green's function, it is clear that if w solves the wave equation,

$$\frac{\partial^2 w}{\partial s^2} = Au + \frac{d}{ds}\phi(s)\chi,$$

for a general function ϕ, then its heat transform solves

$$\frac{\partial u}{\partial t} = Au + \phi(t)\chi,$$

which leads to a way of analysing temperature measurements other than the step-response case.

4. Inversion of the heat transform. Given the observed temperature values $y(t)$ at certain points, we propose to invert the heat transform and look at the corresponding heat wave function w to find out about the internal structure (e.g., location of interfaces) of the package. As this leads to an inversion of an integral equation of the first kind, this is certainly a linear ill-posed problem. Moreover, as the kernel of the integral equation (2.17) is analytic, we expect that it is a severely ill-posed problem. A way to compute approximate solutions $w(s)$ of the equation

(4.1) $$y(t) = \mathcal{H}w(t)$$

is by regularization [7]. There is a large choice of possible methods, that could be applied, such as Tikhonov regularization, and some successful numerical experiment shows that this is possible.

However, when dealing with regularization, the regularization should always be some-how related to the expected solution in order to give good results. Although most of the well-known regularization methods give rise to convergence, the rate of convergence strongly depends on the solution and on the interplay between regularization and solution properties (in abstract form this appears as a source condition [7]).

In the example in the previous section, we saw that for small, localized sources, the wave equation solution is a sum of delta pulses. Thus we can expect that the solution has a sparse structure, i.e., a discretized solution w of (4.1) will only have a small number of nonzero coefficients.

The use of sparsity based regularizations seems to be a promising way in this setting. Recently, a number of algorithms that exploit the sparsity structure have been proposed [4, 19]. Closely related to this is the popular field of compressed sensing [2].

In our case we used the semi-smooth Newton method of Griesse and Lorenz [10], which turned out to be quite fast and reliable. However, we modified their method, by introducing an additional regularization term. As an alternative, the soft-thresholding algorithm of [4] could be used. This has the advantage of being quite stable, but was rather slow in our computations.

Let us describe the algorithm we used: the data $u(t)$ are usually given at discrete time points

$$y = u(t_i)_{i=1}^m.$$

We discretize w as a sum of delta distributions

$$w(s) := \sum_{j=1}^n m_j \delta(s - s_j) \quad m = (m_j)_{j=1}^n.$$

In the discrete setting this leads to a linear equation

$$y = Am$$

with the matrix

$$A_{i,j} = \Phi(\frac{s_j}{2\sqrt{t_i}})$$

The semi-smooth Newton method of [10] seeks a minimizer of the Tikhonov-type functional

$$(4.2) \qquad J(m) = \frac{1}{2}\|Am - y\|^2 + \alpha \sum_{i=1}^m |m_i|.$$

The optimality condition can be written as

$$m - S_{\gamma\alpha}(m - \gamma A^* A(m - y)) = 0$$

for any $\gamma > 0$, using the soft-thresholding operator

$$S_\omega(m) = \text{sign}(m) \max(0, |m| - \omega),$$

where all operations are applied componentwise on m. The algorithm of [10] computes in each iteration a vector m^k, in the following way:

1. Compute the active and inactive indices:

$$\mathcal{A}^k := \{i \in \mathbb{N} \,|\, |m^k - A^*(Am^k - y)|_i > \gamma\alpha\},$$
$$\mathcal{I}^k := \{i \in \mathbb{N} \,|\, |m^k - A^*(Am^k - y)|_i \leq \gamma\alpha\}.$$

2. Compute the residual:

$$r^k = m^k - S_{\gamma\alpha}(m^k - \gamma A^* A(m^k - y)).$$

3. Calculate the Newton update:

$$\begin{bmatrix} \gamma M_{\mathcal{A},\mathcal{A}} & \gamma M_{\mathcal{A},\mathcal{I}} \\ 0 & I_{\mathcal{I}} \end{bmatrix} \begin{bmatrix} \delta m_{\mathcal{A}} \\ \delta m_{\mathcal{I}} \end{bmatrix} = - \begin{bmatrix} \delta r^k_{\mathcal{A}} \\ \delta r^k_{\mathcal{I}} \end{bmatrix}.$$

4. Update

$$m^{k+1} = m^k + \delta m.$$

Here $M_{\mathcal{A},\mathcal{A}}$, and $M_{\mathcal{A},\mathcal{I}}$ are the submatrices of A^*A, corresponding to active and inactive indices. $I_{\mathcal{I}}$ is the identity matrix. Of course, the iteration has to be stopped by a suitable stopping rule; see [10].

Local convergence of the iterates m^k to a minimizer of (4.2) was shown in [10]. One problem, which we encountered is that this iteration might become unstable, as the matrix in step 3 can be ill-conditioned. So we introduced an ad-hoc regularization, and replaced step 3 by

$$\begin{bmatrix} \gamma M_{\mathcal{A},\mathcal{A}} + \beta\gamma I_{\mathcal{A}} & \gamma M_{\mathcal{A},\mathcal{I}} \\ 0 & I_{\mathcal{I}} \end{bmatrix} \begin{bmatrix} \delta m_{\mathcal{A}} \\ \delta m_{\mathcal{I}} \end{bmatrix} = - \begin{bmatrix} \delta r^k_{\mathcal{A}} \\ \delta r^k_{\mathcal{I}} \end{bmatrix},$$

with some small positive parameter β. Furthermore we included a damping factor in the Newton update, such that step 4 was changed to

$$m^{k+1} = m^k + \gamma\delta m.$$

It turned out that this helped to stabilize the problem. In this algorithm, γ acts as a stepsize parameter, and α is a regularization parameter enforcing sparcity, while β is another regularization parameter ensuring stability. They can be found by certain parameter choice rules.

The output of this algorithm is a regularized solution to the discretized problem (4.1). The relation between regularized solution and exact solution to (4.1) can be studied by the standard theory of Tikhonov regularization (e.g., [7, 19]) and (4.2).

5. Numerical examples. The operation of the earlier presented mathematical apparatus was verified for the numerical data, both for simulated and experimentally measured data.

5.1. Test example. We first applied the inversion of the heat transform to synthetic data for a simple geometry to show the wave-like property of the numerically computed heat wave function.

In the first example we considered the heat equation

$$\frac{d}{dt}u = D\Delta u$$

on a cuboid $(x, y, z) \in \Omega = [0, 0.5] \times [0, 0.5] \times [0, 2]$. The heat source is placed at the face $z = 0$ in the form of a Neumann condition

$$\frac{\partial}{\partial n}u = 1, \quad \partial\Omega \cap \{z = 0\}.$$
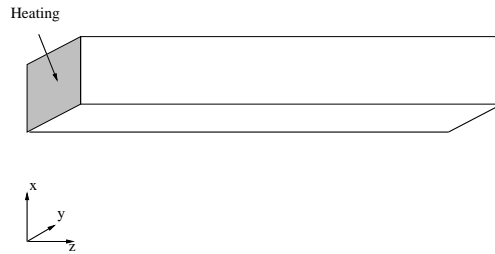
FIG. 5.1. *Test example configuration.*

At $z = 2$, we apply Robin-boundary conditions,

$$\frac{\partial}{\partial n}u = -\frac{1}{2}u, \quad \partial\Omega \cap \{z = 2\},$$

while at all the other parts of the boundary we impose homogenous Neumann conditions $\frac{\partial}{\partial n}u = 0$; see Figure 5.1. For the diffusivity, we set $D = 2$, and the initial conditions were $u = 0$ at $t = 0$. In a weak formulation this problem has the form (2.1). The solution to the heat equation is computed by 3D-FEM using FEMLAB. We consider an observation along one of the lateral faces of the cuboid, at $x = 0$, $y \in [0, 0, 5]$, $z \in [0, 2]$ for a certain time interval until the temperature reaches a steady state at $T \sim 20$.

From these observation data, we computed the corresponding heat wave function by inverting the heat transform using the semi-smooth Newton method from Section 4. For the discretization of s, we used a grid with quadratically increasing spacing, and chose the parameters ($\alpha = 0.6$, $\beta = 0.5$, $\gamma = 0.1$).

The solution to the wave equation is expected to have the following behavior: At $z = 0$ a planar wave is generated at $s = 0$, which travels in the z-direction. When it reaches the boundary at $z = 2$, it is reflected and will move back to $z = 0$, where again reflection will take place, and so on. Because of the shape of Ω, the wave does not depend on x and y, but only on z.

In Figure 5.2 we plotted the result of the heat inversion, i.e., the intensity of the wave function $w(s, x, y, z)$ for different values of s over the coordinate z. It was indeed the case, that the wave function did not depend on x, y in a significant way. In the figure we see that at $s = 0$ a wave is generated which travels in the positive z-direction. The time, at which the boundary $z = 2$ is hit, calculates by (3.8) to $s = \frac{2}{\sqrt{D}} \sim 1.4$. This corresponds to the lower parts of the pictures, where the bottom curve meets the right boundary.

In the picture we also see two separate parts of a wave, which combine at $z \sim 1.5$. We suspect that this is due to reflections close to the source, but it could as well be an artefact due to the ill-posedness.

Later at $s \sim 2.4$, we see a reflected wave, which travels backwards from $z = 2$ to $z = 0$. However, this reflected wave is already smeared out quite a lot, an effect that might again be due to the ill-posedness. High order reflections are not observed any more. We conclude that the heat wave function gives a reasonable good qualitative picture: we can observe a wave traveling from the source to the left and a reflected wave traveling back. The location of the wave peaks at different times and space position is, however, not totally reliable due to the ill-posedness. Note that in this setting it is, of course, much simpler to calculate the wave function directly by solving the wave equation with numerically with finite elements. Our indirect computation via the heat equation solution and the heat transform is done to illustrate the possibility of finding the wave function from the heat equation solution. In a
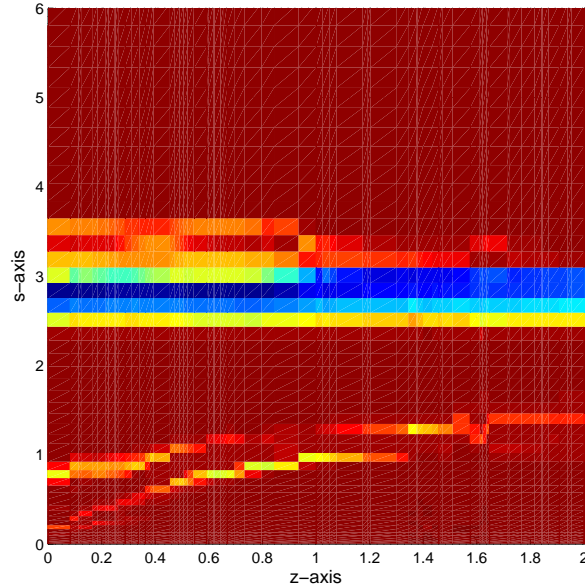
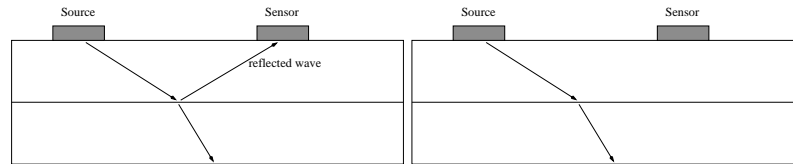FIG. 5.2. *Density of the wave function* $w(s, ., ., z)$.

FIG. 5.3. *Left: high contact resistance induces a reflected wave. Right: Low contact resistance.*

experimental setting, the wave function cannot be computed directly, because the geometry and the parameter are not known.

For the next examples we turned to more realistic data of an electronic circuits for a configuration as in Figure 2.1. The data $y(t)$ used in this verification were both generated by a thermal simulator and measured experimentally. The simulated structure heating curves $y(t)$ were obtained with Fourier series Green's function thermal simulator [1, 11, 16], whereas the measured data were obtained from the transient thermal tester T3Ster® provided by the MicRed company. This equipment allows the registration of thermal transients with the resolution of 1 microsecond and renders possible the analysis of the measurement data employing the method described in [20, 22, 23].

5.2. Finding contact resistance from simulated data. The model equations and boundary conditions were taken from [16]. The aim of the first part was to investigate the impact of increasing the contact resistance between the layers, since this phenomenon was also considered during the measurements of the real circuit. The expected effect of the induced heat wave function is sketched in Figure 5.3. For a low contact resistance (right figure) the wave will travel through, while for a high contact resistance a reflection wave should appear for the heat wave function.

The structure consisted of two layers (1.52mm and 4.00mm thick) made of copper. The heating curves were simulated for a small (10x10 microns) heat source, dissipating 10W, cen-
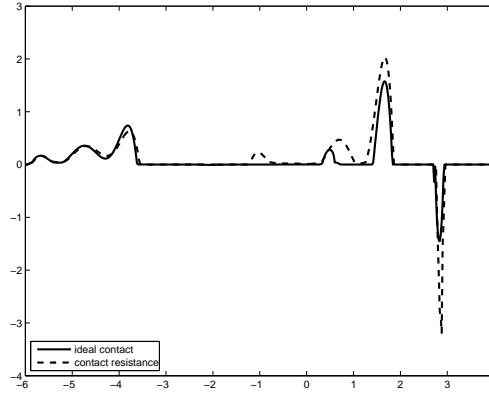
FIG. 5.4. *Effects of contact resistance (simulated data).*

trally located on the top of the thinner layer. Two cases were considered; first it was assumed that the contact between the layers was ideal (full line) and then the contact resistance was increased (dashed line). Simulated logarithmically equidistant time samples were used to compute the heat wave function by the algorithm above. In Figure 5.4 we plotted the result of the semi-smooth Newton method – the heat wave $w(s, x_{obs})$ – on a logarithmic scale (i.e. over $\log(s)$).

As can be seen, the contact resistance increases significantly the height of the peaks located more to the right and forces an additional peak to appear at $\log(s) \sim -1$. This result shows the expected behavior as in Figure 5.3. In the graph for the increased contact resistance (dashed line), the additional peak at $\log(s) \sim -1$ can be interpreted as reflection effect on the interface. Hence, the effect of high/low contact resistance is easily visible in the heat wave picture. But, of course, it is almost impossible to see the corresponding effect directly from the data $y(t)$.

5.3. Finding effect of cooling from experimental data. In Figures 5.6 and 5.7 we show the result of the inversion of the heat transform using experimentally measured data for a circuit model as described in [15]. The purpose of this experiment was to characterize the cooling boundary conditions from experimental data $y(t)$.

Three experiments were performed, in one the heat sink was attached tightly, in the next one, the heat sink was loosened and in a third experiment thermal grease was attached on the interface between package and heat sink. These three experiments only change the boundary conditions on the bottom. The heat wave function should indicate a difference between these cases, as it is reflected differently – in a similar situation as in Figure 5.3 – but now the different reflection happens at the bottom boundary, not between the layers as in the previous example.

Figure 5.6 shows the heat wave function computed from the data on a logarithmic scale $\log(s)$. Here the full line corresponds to the case when the heat sink is attached tightly, in the next one, the heat sink was loosened (dashed-dotted line) and in a third experiment thermal grease was attached on the interface between package and heat sink (dashed line).

Indeed, the figure displays this behavior as expected. We can see a difference in the heat wave solution at $\log(s) \in [0, 3]$. Note that the loose case has the highest peak at $\log(s) \sim 1.1$, compared to the other case. This has the interpretation that the loosening will create the highest reflection of the heat wave, while the other case will conduct the wave in a better way. The thermal grease here shows least reflections, indicating that it has the best thermal
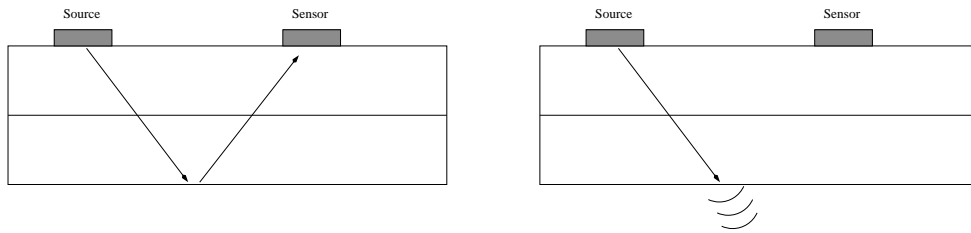
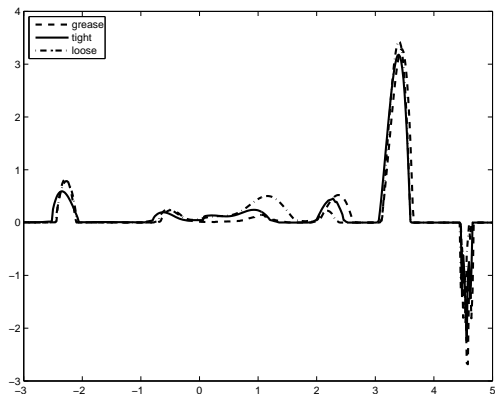FIG. 5.5. *Left: Moderate cooling   Right: Forced cooling.*

FIG. 5.6. *Effects of loosening the heat sink (experimental data).*

conducting properties amongst these three cases.

In Figure 5.7 another experiment was considered. We investigated the effect of cooling at the bottom: Two cases we analyzed: the solid line is the heat wave function for data with forced air cooling at the bootom, while the dashed line corresponds to the same experiment with cooling only by free convection (still air). The difference in the heat equation between these two cases are again only the boundary conditions on the bottom, which have a different heat transfer coefficient involved in either case. A sketch of the expected wave behaviors is seen in Figure 5.5. Different types of cooling will show a different reflected wave. For a high cooling most of the energy will dissipate into the heat sink. For a comparable low cooling some part of the energy will be reflected. The main difference between the two plots is at the right-hand side at $\log(s) \in [1,5]$, while the heat wave function hardly differs for smaller times s. From this picture we conclude that the peaks on the right-hand side starting at $\log(2) \sim 2$ are due to the effects of the heat sink. The peaks at earlier time, e.g., at $\log(s) \sim -2.2, 0$ are due to the reflections at the layers of the material. We see that they are quite the same for both experiments. The most obvious difference is the peak for the free convection cooling (low cooling), which is not there for forced cooling. Again this fits the observation that in the forced cooling case most of the wave energy will dissipate out and little will be reflected.

Note that the first peak on the left at $\log(s) \sim -5$ is the wave that travels directly from the source to the observation point without reflection.

Furthermore in view of equation (3.2) the total gain of temperature should be equal to the integral of the wave function. Indeed, for the experimental cases a summation of the wave functions agreed up to 10% to the total temperature gain.
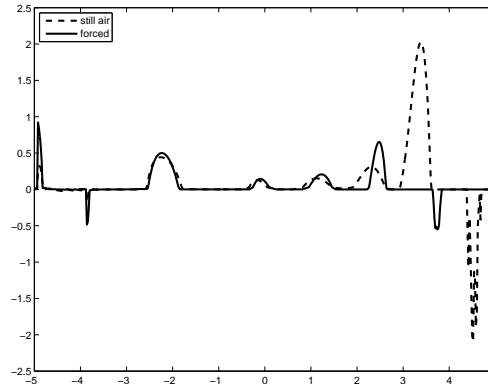
FIG. 5.7. *Effects of blowing air on heat sink (experimental data).*

6. Conclusion and comments. It is obvious from the pictures that the computed heat wave function can be used to classify cooling boundary conditions and interfaces. It gives a qualitative picture of the effects of, e.g., boundaries, interfaces and location of sources. The reason for this is that the wave equation transports this information to the observation point.

From the computed heat wave function we can certainly distinguish cases when the heat sink is not attached properly, or if forced cooling took place and we can compare the thermal quality of an interface. As an possible application this can be used to find, for instance, manufacturing faults by comparing the heat wave function to a reference function.

Note that, once the heat wave function is computed, the comparison can be done by visual inspection, and the regions, where additional peaks occur can be related to the location of interfaces or boundaries in the package by (3.8) (or similar formulae).

This certainly cannot be done just by inspection of the thermal data $y(t)$, because the effects of contact resistance and boundary condition are *not localized* there, while they are in the heat wave function. Furthermore, comparable methods of finding interface or boundary conditions may give a quantitative estimate of parameters, but usually requires multiple time-consuming numerical solutions of the heat equation; in our approach we only have to solve one linear inverse problem.

Moreover, since the time-constant spectrum can be calculated from the heat wave function by (3.3), $w(s)$ determines the thermal input-output behavior of the package. Thus, the heat wave function can be used to characterize and classify the thermal response of a package, replacing or completing the picture, that the time-constant spectrum gives.

We think that this new method of analyzing thermal data can help to better understand thermal properties of electronic systems.

REFERENCES

[1] J. V. BECK, K. D. COLE, A. HAJI-SHEIKH, AND B. LITKOUHI, *Heat Conduction Using Green's Functions*, Taylor & Francis, NY, 1992.
[2] E. CANDÈS AND J. ROMBERG, *Sparsity and incoherence in compressive sampling*, Inverse Problems, 23 (2007), pp. 969–985.
[3] L. CODECASA, *Structure function representation of multidirectional heat-flows*, IEEE Trans. Comp. Pack. Tech., 30 (2007), pp. 643–652.

[4] I. DAUBECHIES, M. DEFRISE, AND C. DE MOL, *An iterative thresholding algorithm for linear inverse problems with a sparsity constraint*, Comm. Pure Appl. Math., 57 (2004), pp. 1413–1457.

[5] J. W. DETTMAN, *The wave, Laplace, and heat equations and related transforms*, Glasg. Math. J., 11 (1970), pp. 117–125.

[6] D. G. DUFFY, *Green's Functions with Applications*, Chapman Hall, Boca Raton, FL, 2001.

[7] H. ENGL, M. HANKE, AND A. NEUBAUER, *Regularization of Inverse Problems*, Kluwer, Dordrecht, 1996.

[8] L. C. EVANS, *Partial Differential Equations*, AMS, Providence, 1998.

[9] I. GRADSHTEYN AND I. RYZHIK, *Table of Integrals, Series, and Products*, Academic Press, San Diego, CA, 1980.

[10] R. GRIESSE AND D. LORENZ, *A semismooth Newton method for Tikhonov functionals with sparsity constraints*, Inverse Problems, 24 (2008), 035007 (19 pages).

[11] A. HAJI-SHEIKH AND J. V. BECK, *Temperature solution in multi-dimensional multi-layer bodies*, Int. J. Heat Mass Tran., 45 (2002), pp. 1865–1877.

[12] L. HÖRMANDER, *The Analysis of Linear Partial Differential Operators. I*, Springer, Berlin, 1990.

[13] V. ISAKOV, *Inverse Problems for Partial Differential Equations*, Springer, New York, 1998.

[14] V. ISAKOV AND S. KINDERMANN, *Identification of the diffusion coefficient in a one-dimensional parabolic equation*, Inverse Problems, 16 (2000), pp. 665–680.

[15] M. JANICKI, J. BANASZCZYK, G. DE MEY, M. KAMINSKI, B. VERMEERSCH, AND A. NAPIERALSKI, *Dynamic thermal modelling of a power integrated circuit with the application of structure functions*, Microelectron. J., 40 (2009), pp. 1135–1140.

[16] M. JANICKI, G. DE MEY, AND A. NAPIERALSKI, *Thermal analysis of layered electronic circuits with Green's functions*, Microelectron. J., 38 (2007), pp. 177–184.

[17] E. N. PROTONOTARIOS AND O. WING, *Theory of nonuniform RC lines, part I*, IEEE Trans. Circ. Syst., 14 (1967), pp. 2–12.

[18] ———, *Theory of nonuniform RC lines, part II*, IEEE Trans. Circ. Syst., 14 (1967), pp. 13–20.

[19] R. RAMLAU AND G. TESCHKE, *A Tikhonov-based projection iteration for nonlinear ill-posed problems with sparsity constraints*, Numer. Math., 104 (2006), pp. 177–203.

[20] V. SZÉKELY, *On representation of infinite-length distributed RC one-ports*, IEEE Trans. Circ. Syst., 38 (1991), pp. 711–719.

[21] ———, *Identification of RC networks by deconvolution: Cances and limits*, IEEE Trans. Circ. Syst., 45 (1998), pp. 244–358.

[22] ———, *Enhancing reliability with thermal transient testing*, Microelectron. Reliab., 42 (2002), pp. 629–640.

[23] V. SZÉKELY AND T. VAN BIEN, *Fine structure of heat flow path in semiconductor devices: A measurement and identification method*, Solid State Electron., 31 (1988), pp. 1363–1368.

[24] D. WIDDER, *Inversion of a heat transform by use of series*, J. Anal. Math., 18 (1967), pp. 389–413.

[25] J. WLOKA, *Partial Differential Equations*, Cambridge University Press, 1987.